frontiers | Frontiers in Chemistry

Vertically ordered mesoporous silica film-assisted electrochemical cytosensor for the sensitive detection of HeLa cells

Zisan Zeng[1], Yang Zhao[1], Luoxing Yang[2], Fengna Xi[2]* and Danke Su[1]*

[1]Guangxi Medical University Cancer Hospital, Guangxi Medical University, Nanning, China, [2]Department of Chemistry, Key Laboratory of Surface and Interface Science of Polymer Materials of Zhejiang Province, Zhejiang Sci-Tech University, Hangzhou, China

Designing fast and simple quantitative methods on cheap and disposable electrodes for the early detection of HeLa cells is highly desirable for clinical diagnostics and public health. In this work, we developed a label-free and sensitive electrochemical cytosensor for HeLa cell detection based on the gated molecular transport across vertically ordered mesoporous silica films (VMSFs) on the disposable indium tin oxide (ITO) electrode. As high affinity for a folate receptor existed on the membrane of HeLa cancer cells, folic acid (FA) functionalized VMSF could regulate the transport of electrochemical probe ($Fe(CN)_6^{3-}$) by the specific recognition and adhesion of HeLa cells toward the VMSF surface. In addition, VMSF, served as a solid skeleton, is able to effectively prevent the direct contact of cells with the underlying electrode, remaining the underlying electrode activity and favoring the diffusion of $Fe(CN)_6^{3-}$. Once specific adhesion of HeLa cells to the VMSF surface happens, $Fe(CN)_6^{3-}$ redox probe exhibits impeded transport in the silica nanochannels, ultimately resulting in the decreased electrochemical responses and realizing the quantitative determination of HeLa cells with a broad linear range (10^1-10^5 cells/mL) and a low limit of detection (4 cells/mL). The proposed electrochemical cytosensor shows a great potential application for the early diagnosis of cervical cancer.

KEYWORDS

vertically ordered mesoporous silica film, cytosensor, HeLa cell, gated molecular transport, electrochemical detection

1 Introduction

As one of the most common gynecological malignancy, cervical cancer has become the lethal cause of death among women in low- and middle-income countries (Feikin et al., 2006). Moreover, carcinoma cells can rapidly grow and spread to the adjacent parts or organs of the body, producing severe impact on women's health. Clinical research indicates that the early detection and treatment of cervical cancer greatly contribute to improving cure rates and survival rates (Hou et al., 2022). At present, histopathological examination of biopsy specimens is the gold standard for the diagnosis of cervical cancer, which can acquire the information about the premalignant and malignant status of the cervix (Kundrod et al., 2019). However, biopsy specimens are obtained in an invasive way, which is inconvenient for

clinical diagnoses (Li et al., 2020b). Morphological imaging technologies, including X-ray computed tomography and magnetic resonance technology, also play an important role for early detection and treatment of cervical cancer (Brindle, 2008). Nevertheless, these detection methods often depend on the expensive large-scale instruments and professional operators along with cumbersome operation steps (Wang et al., 2021). Therefore, it is particularly important to develop fast and sensitive detection methods for cervical cancer.

HeLa cells closely associated with cervical cancer are extremely important, and their content is helpful for the diagnosis and therapy of patients with cervical cancer (Gansukh et al., 2019). Traditional detection methods for HeLa cells include polymerase chain reaction (Lin et al., 2019), colorimetry (Chen et al., 2015; Teng et al., 2019), electrochemiluminescence (ECL) (Zhang et al., 2018), electrochemistry (Liu et al., 2021; Hu et al., 2022), photoelectrochemistry (Fan et al., 2019), and fluorometry (Guo et al., 2014). Electrochemical biosensors is equipped with prompt response, high sensitivity, and easy miniaturization, which has become one of the most powerful analytical techniques for complex biological samples (Gong et al., 2022a; Cui et al., 2023). In general, the specific recognition and electrochemical detection of cancer cells are accomplished by the utilization of tumor markers [folate receptor (FR), glycan receptors, and growth factor receptor] (Soleymani et al., 2020) or aptamer (Zhang et al., 2017). FR, as a kind of glycosyl-phosphatidylinositol-anchored cell-surface glycoprotein (O'Shannessy et al., 2012; Scaranti et al., 2020), will overexpress on the membrane of HeLa cells while limitedly express on that of normal cells, which has high affinity for folic acid (FA) (Scaranti et al., 2020). On the basis of the aforementioned case, FA has often been used as the recognition element to construct various electrochemical cytosensors for the detection of HeLa cells(Soleymani et al., 2018).

Vertically ordered mesoporous silica films (VMSFs) possessing ultrathin, ultrasmall and uniform pore size, perpendicularly aligned nanochannels, and high porosity are potential to provide high permeability and selectivity with respect to the size, charge, lipophilicity, and structure, which have attracted particular attention in the field of electrochemical analysis (Yan et al., 2020a; Ma et al., 2020; Yan et al., 2021; Han et al., 2022; Deng et al., 2023; Huang et al., 2023). With a high density of silanol groups on the silica walls, VMSF can either exhibit an electrostatic effect for the confinement of electrochemical/ECL probes (Gong et al., 2022b; Gong et al., 2022c; Zhou et al., 2023) inside the nanochannels or provide functional sites for the immobilization of specific recognition elements [e.g., antibody (Ma et al., 2022a; Ma et al., 2022b; Chen et al., 2022], aptamer (Wu et al., 2015; Zhang et al., 2023), and phenylboronic acid (Yan et al., 2020b) on the surface, which is able to construct various electrochemical/ECL sensors based on the surface-confined probes or the gated molecular transport of probes in solution across the silica nanochannels of VMSF (namely, "turn on" or "turn off" strategies) (Huang et al., 2022; Luo et al., 2022). In comparison with the immobilization of probes on the electrode surface, probes in solution combined with recognition element functionalized VMSF could realize all electrochemical reactions in a homogeneous solution without the complex electrode

modification process. Moreover, compared to the antibody and aptamer, FA that served as the recognition element has a small size and long-term good stability, as well as high recognized ability for FR overexpressed on cancer cells (Xu et al., 2013). To the best of our knowledge, the utilization of FA functionalized VMSF for the electrochemical analysis of cancer cells has not been reported yet.

In this work, we report folic acid (FA) functionalized VMSF for highly sensitive and label-free determination of HeLa cells based on the gated transport of electrochemical redox ($Fe(CN)_6^{3-}$) across the nanochannels of VMSF. Cheap and disposable ITO electrodes are employed as the supporting electrode to stably grow VMSF. As high affinity for FR existed on the membrane of HeLa cancer cells, FA can be covalently immobilized on the VMSF surface by using EDC/NHS coupling agents. Once HeLa cells are specifically recognized and attached to the VMSF surface, the impeded transport of $Fe(CN)_6^{3-}$ in the silica nanochannels occurs, leading to the diminished electrochemical signals related to the concentration of HeLa cell. The quantitative analysis of HeLa cells can be realized by recording the DPV signals, and the fabricated electrochemical cytosensor with good biocompatibility shows a great potential application in the early diagnosis of cervical cancer.

2 Materials and methods

2.1 Chemicals and materials

Tetraethyl orthosilicate (TEOS), 3-aminopropyltriethoxysilane (APTES), hexadecyltrimethylammonium bromide (CTAB), potassium ferricyanide (K_3 [$Fe(CN)_6$]), potassium ferrocyanide (K_4 [$Fe(CN)_6$]), sodium phosphate dibasic dodecahydrate ($Na_2HPO_4 \bullet 12H_2O$), potassium hydrogen phthalate (KHP), bovine serum albumin (BSA), folic acid (FA), 1-ethyl-3-(3-dimethylaminopropyl)carbodiimide (EDC) N-hydroxysuccinimide (NHS), glucose (Glu), sodium chloride (NaCl), dopamine (DA), and ascorbic acid (AA) were all purchased from Aladdin Chemistry Co. Ltd., (China). Potassium chloride (KCl) and ethanol (EtOH) were ordered from Hangzhou Gaojingchem (China). L-alanine and sodium dihydrogen phosphate dehydrate ($Na_2H_2PO_4 \bullet 2H_2O$) were obtained from Macklin (China). PBS (0.01 M) was prepared by mixing $Na_2HPO_4 \bullet 12H_2O$ and $NaH_2PO_4 \bullet 2H_2O$ into ultrapure water. Ultrapure water (18.2 MΩ cm) obtained from a Millipore water purification system was used to prepare all solutions. Therefore, all reagents used in the experiment were of analytical grade without further treatment. ITO-coated glasses were purchased from Zhuhai Kavio Optoelectronic Technology (China).

2.2 Apparatus and characterization

A transmission electron microscope (HT7700, Hitachi, Japan) was used to characterize the surface morphology of VMSF. VMSF was scraped moderately from the ITO electrode surface and subsequently dissolved in EtOH to obtain the transmission electron microscopy (TEM) specimen, which could be employed for the TEM observation operated at 100 kV. The Autolab electrochemical workstation (PGSTAT302N, Metrohm,

Switzerland) was utilized to carry out all electrochemical experiments including cyclic voltammetry (CV) and differential pulse voltammetry (DPV). The scan rate for CV tests was 50 mV/s, and the parameters for DPV tests were as follows: step, 0.005 V; modulation amplitude, 0.025 V; modulation time, 0.05 s; and interval time, 0.2 s.

2.3 Modification of vertically ordered mesoporous silica films on the indium tin oxide electrode

The pretreatment of bare ITO was necessary to remove the impurity from the electrode surface and improve the hydrophilicity of the electrode surface for further VMSF growth. Briefly, bare ITO electrodes (5 cm × 0.5 cm) were soaked into NaOH (1 M) overnight and treated successively with acetone, ethanol, and deionized water under ultrasonication for 30 min. VMSF with good biocompatibility was grown onto the cleaned bare ITO electrodes by using electrochemically assisted self-assembly (EASA) approach as previously reported (Zhang et al., 2022; Zhou et al., 2022; Zou et al., 2022). The directly obtained electrode remains templated surfactant micelles (SM), termed as SM@VMSF/ITO. To remove SM from the silica nanochannels, HCl-EtOH (0.1 M) was employed and VMSF/ITO electrode was acquired.

2.4 Preparation of folic acid-aminopropyltriethoxysilane/vertically ordered mesoporous silica films/indium tin oxide electrode

FA with high affinity for FR existed on the membrane of HeLa cancer cells was functionalized on the surface of VMSF according to the previous literature with a slight adjustment (Li et al., 2020a), which is involved in the synthesis of FA functionalized with APTES (FA-APTES) and its covalent modification to the VMSF. First, FA (40 mg), EDC (20 mg), and NHS (30 mg) were dissolved into DMSO (2 mL) and stirred in the dark for 30 min to activate the carboxyl groups of FA and form NHS ester. APTES (125 μL) was then added to the aforementioned activated FA solution under stirring for 2 h to replace the active NHS esters, eventually resulting in the formation of the FA-APTES complex. Subsequently, the VMSF/ITO electrode was placed into EtOH (10 mL) containing FA-APTES (400 μL) and reacted for another 2 h. After being rinsed thoroughly with EtOH to remove unreacted FA-APTES, FA-APTES-modified VMSF on the ITO electrode was obtained called FA-APTES/VMSF/ITO.

2.5 Cell culture

HeLa cells were cultured in Dulbecco's Modified Eagle Medium (DMEM) supplemented with fetal bovine serum (FBS, 10%) at 37°C in a humidified atmosphere containing CO_2 (5%). The cells were trypsinized and subcultured every 2 days. The cell number was detected using a Petroff-Hausser cell counter.

2.6 Electrochemical determination of HeLa cells

The cells were separated from the medium by centrifugation at 2,000 rpm for 3 min and then washed twice with sterile PBS. The sediment was carefully redispersed in PBS to obtain a homogeneous HeLa cell suspension at a certain concentration. Then, the FA-APTES/VMSF/ITO electrode was incubated with various concentrations of HeLa cell suspension for 20 min. The steric hindrance effect produced in the recognition process inhibits the mass transfer of the probe through bulk solution to the underlying ITO electrode, leading to the reduction of the electrochemical signal and further realizing the detection of HeLa.

3 Results and discussion

3.1 The construction of the electrochemical cytosensor

Figure 1 shows the fabrication of VMSF-assisted electrochemical cytosensor for HeLa cell detection. As shown, ITO modified with VMSF (VMSF/ITO) was first obtained by using the EASA method and subsequent removal of SM, which could provide a gated-controlled electrode substrate for FA-APTES cross-linking and further HeLa cell recognition. Due to the amino groups of APTES and carboxyl groups of FA, FA could be functionalized with APTES through EDC/NHS activated agents, followed by modification to the surface of VMSF/ITO through the silanization reaction. Thus, FA possessing high affinity to FR-riched HeLa cells has been successfully grafted to the sensing interface, and the obtained sensor was termed as FA-APTES/VMSF/ITO. Benefiting from the overexpression of FR on the membrane of HeLa cells, HeLa cell could be specifically recognized by the proposed FA-APTES/VMSF/ITO sensor and attached to the electrode surface, producing a steric hindrance effect and eventually inhibiting the access of the electrochemical redox probe $(Fe(CN)_6^{3-})$ to the underlying ITO electrode. Therefore, the reduced electrochemical signals have a relation to the concentration of HeLa cells, allowing the quantitative determination of Hela cells. It should be noted that VMSF acting as a solid skeleton is capable of preventing the direct contact of cells with the underlying electrode, effectively maintaining the electrode activity and effective diffusion of the probe.

3.2 Morphology and electrochemical characterization of vertically ordered mesoporous silica films

The pore size and thickness of VMSF could first be confirmed from the top-view and cross-sectional TEM images shown in Figures 2A,B. It can be seen that the prepared VMSF with hexagonally oriented pores is intact without large defects, and the parallel nanochannels are in long-range order. The diameter and thickness are approximately 2–3 nm and 160 nm, respectively. Electrochemical strategies including CV and EIS were used to
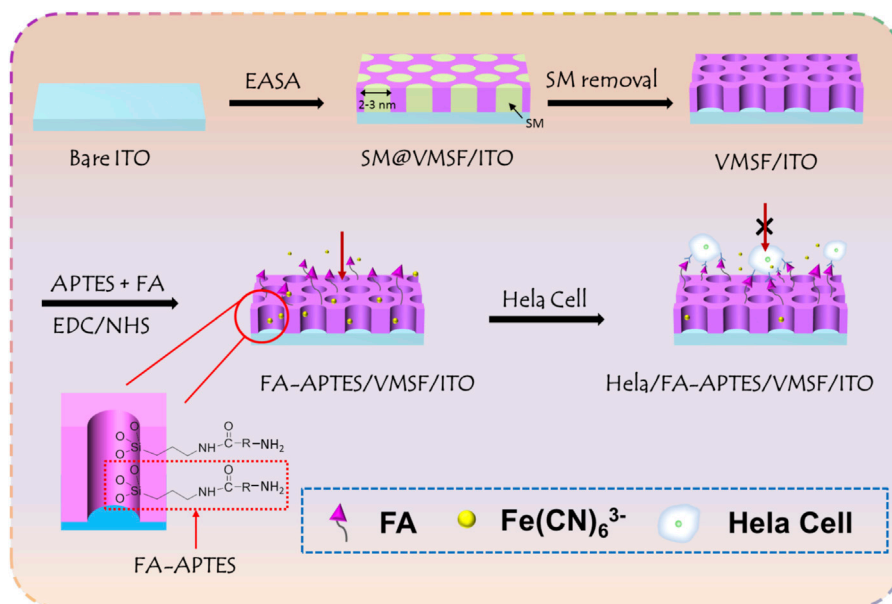
FIGURE 1
Schematic illustration for the fabrication of VMSF-assisted electrochemical cytosensor for HeLa cell detection.
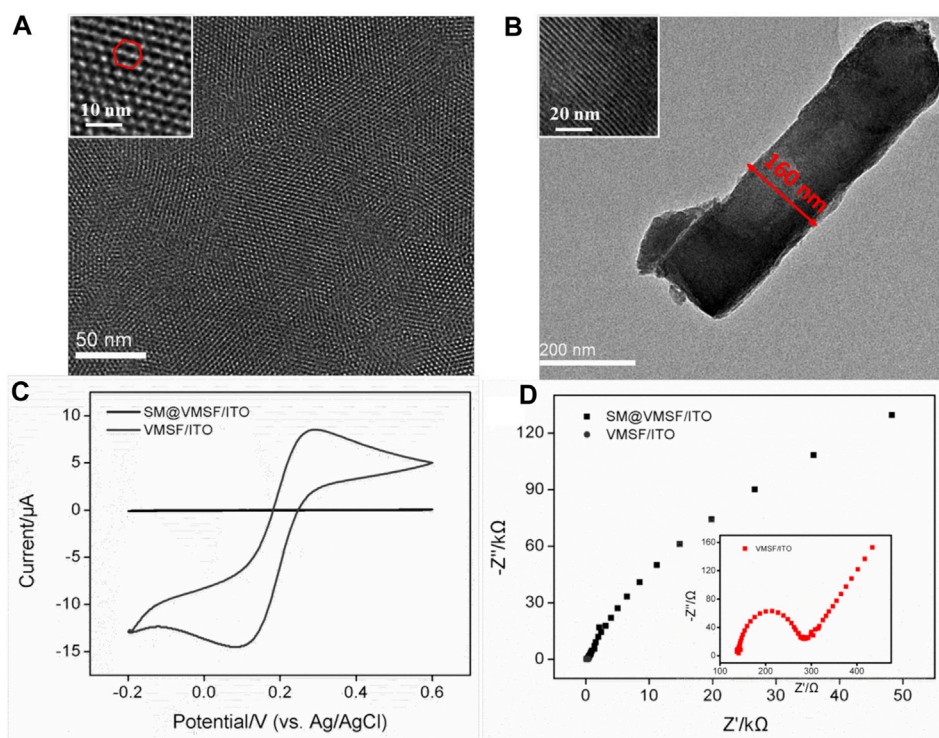

FIGURE 2
(A) Top-view and **(B)** cross-sectional TEM images of VMSF. Insets in **(A)** and **(B)** display the corresponding amplified TEM images. **(C)** CV curves obtained at the SM@VMSF/ITO and VMSF/ITO electrodes in KHP (0.05 M) solution containing Fe(CN)$_6^{3-}$ (0.5 mM). **(D)** Nyquist plots of SM@VMSF/ITO and VMSF/ITO electrodes obtained in a KCl (0.1 M) solution containing K$_3$Fe(CN)$_6$/K$_4$Fe(CN)$_6$ (2.5 mM).
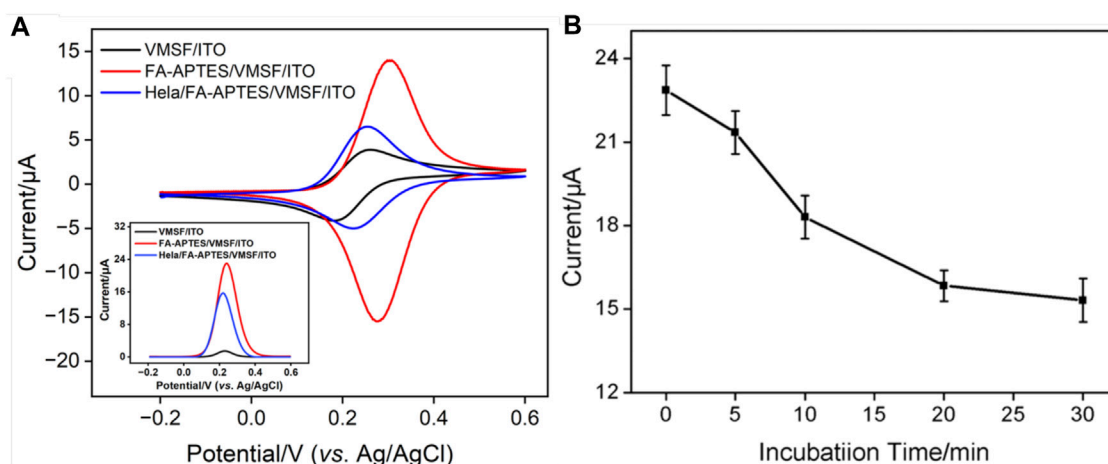
FIGURE 3
(A) CV curves of VMSF/ITO, FA-APTES/VMSF/ITO, and HeLa/FA–APTES/VMSF/ITO electrodes in KCl (0.1 M) solution containing $Fe(CN)_6^{3-}$ (0.05 mM). Inset is the corresponding DPV curves. **(B)** Optimization of the incubation time for HeLa cells on the proposed FA-APTES/VMSF/ITO cytosensor. Concentrations of $Fe(CN)_6^{3-}$ or HeLa cells are 0.05 mM and 10^4 cells/mL.

survey the integrity and permeability of VMSF. Figures 2C,D show that the SM@/VMSF/ITO electrode only displays charging currents and a large charge transfer resistance (Rct), which is attributed to the hydrophobic environment inside the nanochannels of VMSF formed by templated SM and further implies that the as-prepared VMSF is unbroken. Upon SM removal, the entrance of $Fe(CN)_6^{3-}$ through the silica nanochannels is unhindered and its redox reaction occurs at the underlying ITO electrode surface, exhibiting a pair of reversible redox peaks in the CV curve and a minor R_{ct} in the Nyquist plot. This is because the open nanochannels of VMSF assembled on the ITO electrode are beneficial for charge transfer. Previous results indicate the successful preparation of VMSF attached to the ITO electrode surface, giving rise to the suitable electrode interface for the immobilization of specific recognition element and cell adhesion.

3.3 Construction of the proposed electrochemical cytosensor

The cytosensor interface was constructed using FA as a recognition element. Figure 3A shows the CV curves of VMSF/ITO, FA-APTES/ VMSF/ITO and HeLa/FA-APTES/VMSF/ITO electrodes in KCl (0.1 M) solution containing $Fe(CN)_6^{3-}$ (0.05 mM). It could be found that a pair of reversible redox peaks corresponding to the electrochemical reaction of $Fe(CN)_6^{3-}$ is displayed at the VMSF/ITO electrode. After the modification of FA-APTES composite on the VMSF surface, the redox peak currents are significantly increased, which is attributed to the electrostatic effect by protonated amino groups on the FA-APTES composite. Once HeLa cells are identified by the FA-APTES/VMSF/ITO cytosensor, the redox peak currents remarkably decrease, which is due to the steric hindrance effect generated by cells

FIGURE 4
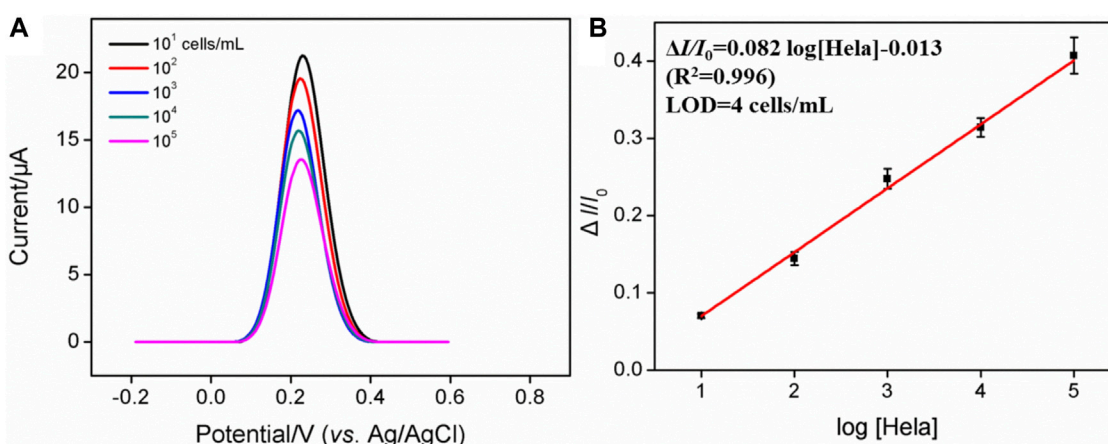**(A)** DPV curves of the FA-APTES/VMSF/ITO cytosensor in 0.05 mM K_3 [Fe(CN)$_6$] and containing different concentrations of HeLa cells. Concentration range is 10^1–10^5 cells/mL. **(B)** Corresponding calibration curves for the detection of HeLa cells.

TABLE 1 Comparison with the existing electroanalytical techniques for the detection of HeLa cells.

Strategy	Technique	Incubation time (min)	Linear range (cells/mL)	LOD (cells/mL)	Refs.
FA/Pt@BSA[1]/AuE	DPV	120	$28-2.8 \times 10^6$	9	Hu et al. (2022)
FA/MUA[2]/Au/GE[3]	EIS	/	$6-10^5$	6	Wang et al. (2012)
FA/PAMAM[4]/Glu[5]/Cys[6]/AuNP/GCPE[7]	CV	60	10^2-10^6	100	Tepeli et al. (2015)
FA@UiO-66[8]/GE	EIS	60	10^2-10^6	90	Du et al. (2019)
FA films/PAH[9]/ITO	EIS	60	$50-10^6$	4	Correia et al. (2021)
	CV		10^2-10^5	19	
FA/MUA/Au/BDD[10]	EIS	20	10^1-10^5	10	Weng et al. (2011)
FA-APTES/VMSF/ITO	DPV	20	10^1-10^5	4	This work

[1]Bovine serum albumin.
[2]11-Mercaptoundecanoic acid.
[3]Gold electrode.
[4]C12 dendrimer generation 4 solution.
[5]Glutaraldehyde.
[6]Cysteamine.
[7]Glassy carbon paste electrode.
[8]Zirconium MOFs.
[9]Poly(allylamine) hydrochloride.
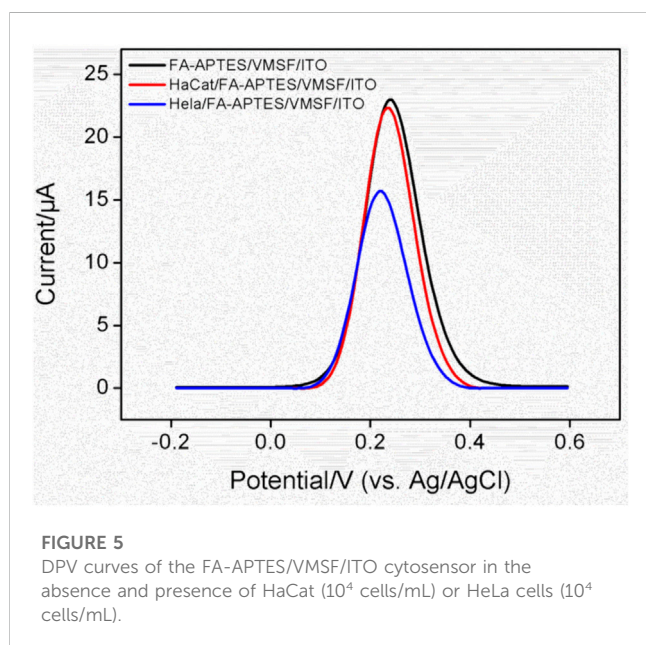[10]Boron-doped diamond.

FIGURE 5
DPV curves of the FA-APTES/VMSF/ITO cytosensor in the absence and presence of HaCat (10^4 cells/mL) or HeLa cells (10^4 cells/mL).

attached to the electrode surface and the inhibited mass transfer of $Fe(CN)_6^{3-}$. The corresponding DPV curves are shown in the inset of Figure 3A, proving the successful construction of our FA-APTES/VMSF/ITO cytosensor.

3.4 Condition optimization of the proposed electrochemical cytosensor

As experimental condition has a crucial impact on the electrochemical performance of the fabricated FA-APTES/VMSF/ITO cytosensor, the incubation time for HeLa cells is optimized.

Figure 3B shows the electrochemical responses at the FA-APTES/VMSF/ITO electrode under various incubation time periods for HeLa cells. It could be found that the anodic peak current of $Fe(CN)_6^{3-}$ depletes with an increase in the incubation time, and no evident variation is observed after 20 min, suggesting that HeLa cells have fully reacted with the binding site of the FA-APTES/VMSF/ITO electrode. Therefore, 20 min is considered as the appropriate incubation time in the following study. Moreover, the kinetic of the $Fe(CN)_6^{3-}$ reaction at the VMSF/ITO electrode was studied, and the results were shown in Supplementary Figure S1. As seen, the equilibrium time is 20 min, which is enough for the binding of HeLa cells on the FA-APTES/VMSF/ITO electrode.

3.5 Determination of HeLa cells

Figure 4 shows that when 0.05 mM $Fe(CN)_6^{3-}$ is present, the dynamic concentration range is from 10^1 to 10^5 cells/mL, and the obtained linear regression equation is $\Delta I/I_0 = 0.082 \log [\text{HeLa}]$ (cells/mL)-0.013 ($R^2 = 0.996$) with a limit of detection (LOD) of four cells/mL. (ΔI and I_0 are defined as $\Delta I = I_{FA}-I_{Hela}$ and I_{FA}, respectively; I_{FA} and I_{Hela} represent the current values of the developed cytosensor before and after the incubation with various concentrations of HeLa cells). As displayed in Supplementary Figure S2, when the concentration of $Fe(CN)_6^{3-}$ is 0.5 mM, the dynamic concentration range is from 10^2 to 10^6 cells/mL, and the obtained linear regression equation is $\Delta I/\Delta I_0 = 0.17 \log [\text{HeLa}]$ (cells/mL)-0.0042 ($R^2 = 0.991$) with an LOD of 12 cells/mL. On the contrary, a high concentration of $Fe(CN)_6^{3-}$ is able to produce the linear range at the high concentration range, while the low concentration of $Fe(CN)_6^{3-}$ generates high sensitivity and low LOD, which is more suitable for practical applications. Table 1 shows the comparison between previously reported electrochemical cytosensors with our developed FA-APTES/VMSF/ITO cytosensor. By contrast, our proposed electrochemical cytosensor is timesaving and has good detection performances in terms of a wide linear range and a low LOD.
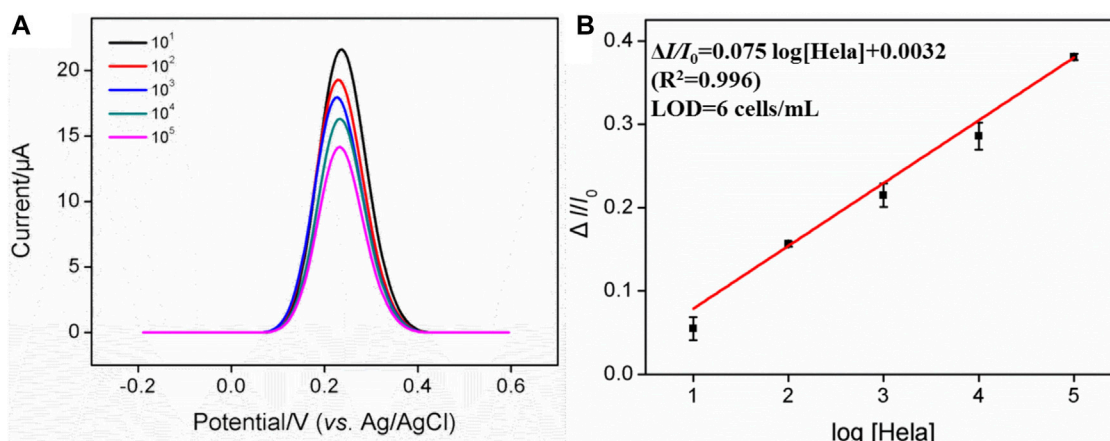
FIGURE 6
(A) DPV curves of the FA-APTES/VMSF/ITO cytosensor in 0.05 mM K_3 [Fe(CN)$_6$] containing 10^3 cells/mL HaCat cells and different concentrations (10^1–10^5 cells/mL) of HeLa cells. **(B)** Calibration curve for the detection of HeLa cells.
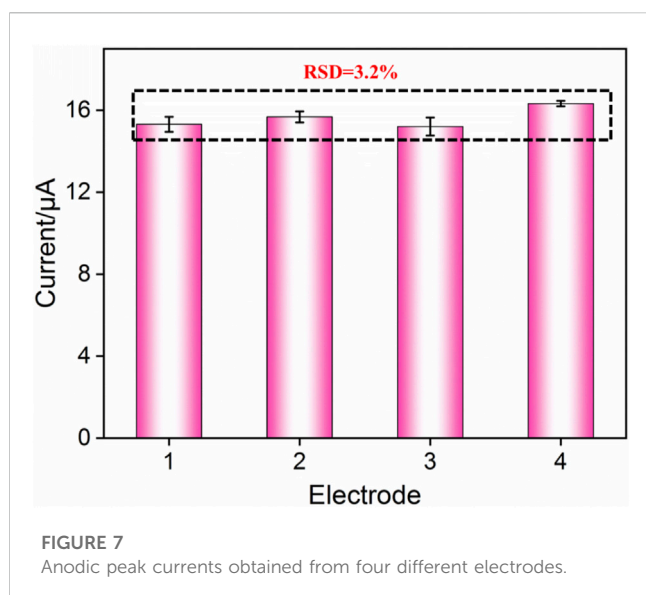

FIGURE 7
Anodic peak currents obtained from four different electrodes.

3.6 Selectivity of the electrochemical cytosensor

The effect of potentially co-existed interfering substances including glucose (Glu), Na^+, K^+, Cl^-, dopamine (DA), ascorbic acid (AA), alanine, and BSA, on the detection of HeLa cells was first evaluated using the FA-APTES/VMSF/ITO cytosensor. As shown in Supplementary Figure S3, only HeLa cells can produce an apparent signal at the FA-APTES/VMSF/ITO cytosensor. Then, selectivity of the fabricated FA-APTES/VMSF/ITO cytosensor was evaluated by comparing the DPV response of the normal cell (HaCat cell). Figure 5 shows the DPV curves of the FA-APTES/VMSF/ITO cytosensor toward the same concentration of HaCat cell and HeLa cell. As displayed, no evident anodic peak current variation is observed for the HaCat cell, while an evident decreased current for the HeLa cell is observed, demonstrating the excellent selectivity of the as-prepared FA-APTES/VMSF/ITO cytosensor.

To further examine the ability of the FA-APTES/VMSF/ITO cytosensor to distinguish between cancer cells and normal cells, HeLa cells with different concentrations were determined in the presence of HaCat cells, and the results were shown in Figure 6. As presented, in the range from 10 to 105 cells/mL, the anodic peak current gradually decreases with the increasing concentration of HeLa cells, and the fitting linear regression equation is $\Delta I/I_0$ = 0.075 log [HeLa] (cells/mL) + 0.0032 (R^2 = 0.996). Hence, the LOD is calculated as six cells per mL. The sensitivity for the detection of HeLa cells in the presence of HaCat cells is very close to that in buffer solution, further indicating that the FA-APTES/VMSF/ITO cytosensor fabricated in this work has high selectivity. However, our proposed cytosensor could not distinguish a specific kind of cell.

3.7 Reproducibility and stability of the electrochemical cytosensor

The reproducibility of the FA-APTES/VMSF/ITO electrochemical cytosensor was assessed by testing four sensors prepared in parallel. Figure 7 shows the relative standard deviation (RSD) of current values obtained from these four cytosensors in the presence of 10^4 cells/mL HeLa cells is 3.8%, confirming that the as-prepared FA-APTES/VMSF/ITO cytosensor has satisfactory reproducibility. Moreover, after a 20-day storage, the developed FA-APTES/VMSF/ITO cytosensor still shows a stable signal for the detection of 10^4 cells/mL HeLa cells.

4 Conclusion

In summary, a label-free and sensitive electrochemical cytosensor for HeLa cells has been constructed by grafting FA to the VMSF surface. FA has high affinity for FR on the membrane of HeLa cells and is able to confer VMSF with specific recognition capacity. When HeLa cells are specifically attached to the VMSF surface, the diffusion of $Fe(CN)_6^{3-}$ through the silica nanochannel is

excluded, leading to the decreased electrochemical response and further allowing the quantitative analysis of HeLa cells with a wide concentration range and a low LOD. Furthermore, the fabricated electrochemical cytosensor has good selectivity, reproducibility, and biocompatibility, which presents a great potential application for the early diagnosis of cervical cancer.

Data availability statement

The raw data supporting the conclusion of this article will be made available by the authors, without undue reservation.

Author contributions

Funding

Conflict of interest

The authors declare that the research was conducted in the absence of any commercial or financial relationships that could be construed as a potential conflict of interest.

Publisher's note

All claims expressed in this article are solely those of the authors and do not necessarily represent those of their affiliated organizations, or those of the publisher, the editors, and the reviewers. Any product that may be evaluated in this article, or claim that may be made by its manufacturer, is not guaranteed or endorsed by the publisher.

Supplementary material

The Supplementary Material for this article can be found online at: https://www.frontiersin.org/articles/10.3389/fchem.2023.1222067/full#supplementary-material

References

Brindle, K. (2008). New approaches for imaging tumour responses to treatment. *Nat. Rev. Cancer* 8, 94–107. doi:10.1038/nrc2289

Chen, D., Li, B., Jiang, L., Duan, D., Li, Y., Wang, J., et al. (2015). Highly efficient colorimetric detection of cancer cells utilizing Fe-MIL-101 with intrinsic peroxidase-like catalytic activity over a broad pH range. *RSC Adv.* 5, 97910–97917. doi:10.1039/c5ra18115a

Chen, H., Huang, J., Zhang, R., and Yan, F. (2022). Dual-mode electrochemiluminescence and electrochemical sensor for alpha-fetoprotein detection in human serum based on vertically ordered mesoporous silica films. *Front. Chem.* 10, 1023998. doi:10.3389/fchem.2022.1023998

Correia, A. R., Sampaio, I., Comparetti, E. J., Vieira, N. C. S., and Zucolotto, V. (2021). Detecting cancer cells with a highly sensitive LbL-based biosensor. *Talanta* 233, 122506. doi:10.1016/j.talanta.2021.122506

Cui, Y., Zhang, S., Zhou, X., Yan, F., and Hu, W. (2023). Silica nanochannel array on co-electrodeposited graphene-carbon nanotubes 3D composite film for antifouling detection of uric acid in human serum and urine samples. *Microchem. J.* 190, 108632. doi:10.1016/j.microc.2023.108632

Deng, X., Lin, X., Zhou, H., Liu, J., and Tang, H. (2023). Equipment of vertically-ordered mesoporous silica film on electrochemically pretreated three-dimensional graphene electrodes for sensitive detection of methidazine in urine. *Nanomaterials* 13, 239. doi:10.3390/nano13020239

Du, L., Chen, W., Wang, J., Cai, W., Kong, S., and Wu, C. (2019). Folic acid-functionalized zirconium metal-organic frameworks based electrochemical impedance biosensor for the cancer cell detection. *Sens. Actuators B Chem.* 301, 127073. doi:10.1016/j.snb.2019.127073

Fan, G., Li, Z., Lu, Y., Ma, L., Zhao, H., and Luo, X. (2019). Robust photoelectrochemical cytosensor in biological media using antifouling property of zwitterionic peptide. *Sens. Actuators B Chem.* 299, 126996. doi:10.1016/j.snb.2019.126996

Feikin, D. R., Flannery, B., Hamel, M. J., Stack, M., and Hansen, P. M. (2006). Vaccines for children in low-and middle-income countries. *Reproductive, Maternal, Newborn, Child Health Dis. Control Priorities* 2, 187–205. doi:10.1596/978-1-4648-0348-2_ch10

Gansukh, E., Nile, A., Sivanesan, I., Rengasamy, K. R. R., Kim, D. H., Keum, Y. S., et al. (2019). Chemopreventive effect of β-cryptoxanthin on human cervical carcinoma (HeLa) cells is modulated through oxidative stress-induced apoptosis. *Antioxidants* 9, 28. doi:10.3390/antiox9010028

Gong, J., Tang, H., Wang, M., Lin, X., Wang, K., and Liu, J. (2022a). Novel three-dimensional graphene nanomesh prepared by facile electro-etching for improved electroanalytical performance for small biomolecules. *Mat. Des.* 215, 110506. doi:10.1016/j.matdes.2022.110506

Gong, J., Zhang, T., Chen, P., Yan, F., and Liu, J. (2022b). Bipolar silica nanochannel array for dual-mode electrochemiluminescence and electrochemical immunosensing platform. *Sens. Actuators B Chem.* 368, 132086. doi:10.1016/j.snb.2022.132086

Gong, J., Zhang, T., Luo, T., Luo, X., Yan, F., Tang, W., et al. (2022c). Bipolar silica nanochannel array confined electrochemiluminescence for ultrasensitive detection of SARS-CoV-2 antibody. *Biosens. Bioelectron.* 215, 114563. doi:10.1016/j.bios.2022.114563

Guo, Y., Sun, G., Zhang, L., Tang, Y., Luo, J., and Yang, P. (2014). Multifunctional optical probe based on gold nanorods for detection and identification of cancer cells. *Sens. Actuators B Chem.* 191, 741–749. doi:10.1016/j.snb.2013.10.027

Han, Q., Zhang, T., Wang, M., Yan, F., and Liu, J. (2022). Disposable electrochemical sensors for highly sensitive detection of chlorpromazine in human whole blood based on the silica nanochannel array modified screen-printed carbon electrode. *Molecules* 27, 8200. doi:10.3390/molecules27238200

Hou, X., Shen, G., Zhou, L., Li, Y., Wang, T., and Ma, X. (2022). Artificial intelligence in cervical cancer screening and diagnosis. *Front. Oncol.* 12, 851367. doi:10.3389/fonc.2022.851367

Hu, C., Wei, G., Zhu, F., Wu, A., Luo, L., Shen, S., et al. (2022). Platinum-based nanocomposite Pt@BSA as an efficient electrochemical biosensing interface for rapid and ultrasensitive de-termination of folate receptor-positive tumor cells. *ACS Appl. Bio Mat.* 5, 3038–3048. doi:10.1021/acsabm.2c00332

Huang, J., Zhang, T., Dong, G., Zhu, S., Yan, F., and Liu, J. (2022). Direct and sensitive electrochemical detection of bisphenol A in complex environmental samples using a simple and convenient nanochannel-modified electrode. *Front. Chem.* 10, 900282. doi:10.3389/fchem.2022.900282

Huang, J., Zhang, T., Zheng, Y., and Liu, J. (2023). Dual-mode sensing platform for cancer antigen 15-3 determination based on a silica nanochannel array using electrochemiluminescence and electrochemistry. *Biosensors* 13, 317. doi:10.3390/bios13030317

Kundrod, K. A., Smith, C. A., Hunt, B., Schwarz, R. A., Schmeler, K., and Richards-Kortum, R. (2019). Advances in technologies for cervical cancer detection in low-resource settings. *Expert. Rev. Mol. diagn.* 19, 695–714. doi:10.1080/14737159.2019.1648213

Li, S., Zhang, P., Dou, L., Wang, Y., Sun, K., Zhang, X., et al. (2020b). Detection of circulating tumor cells in breast cancer patients by nanopore sensing with aptamer-mediated amplification. *ACS Sens.* 5, 2359–2366. doi:10.1021/acssensors.9b02537

Li, S., Zhang, Y., He, X. W., Li, W. Y., and Zhang, Y. K. (2020a). Multifunctional mesoporous silica nanoplatform based on silicon nanoparticles for targeted two-photon-excited fluorescence imaging-guided chemo/photodynamic synergetic therapy *in vitro*. *Talanta* 209, 120552. doi:10.1016/j.talanta.2019.120552

Lin, J., Chen, L., Jiang, W., Zhang, H., Shi, Y., and Cai, W. (2019). Rapid detection of low-level HeLa cell contamination in cell culture using nested PCR. *J. Cell Mol. Med.* 23, 227–236. doi:10.1111/jcmm.13923

Liu, L., Wu, D., Zhen, S., Lu, K., Yi, X., and Sun, Z. (2021). Electrochemical detection of telomerase in cancer cells based on the *in-situ* formation of streptavidin-biotin-DNA-biotin networks for signal amplification. *Sens. Actuators B Chem.* 334, 129659. doi:10.1016/j.snb.2021.129659

Luo, X., Zhang, T., Tang, H., and Liu, J. (2022). Novel electrochemical and electrochemiluminescence dual-modality sensing platform for sensitive determination of antimicrobial peptides based on probe encapsulated liposome and nanochannel array electrode. *Front. Nutr.* 9, 962736. doi:10.3389/fnut.2022.962736

Ma, K., Luo, X., Wu, W., and Liu, J. (2022b). Fabrication of a disposable electrochemical immunosensor based on nanochannel array modified electrodes and gated electrochemical signals for sensitive determination of C-reactive protein. *Nanomaterials* 12, 3981. doi:10.3390/nano12223981

Ma, K., Zheng, Y., An, L., and Liu, J. (2022a). Ultrasensitive immunosensor for prostate-specific antigen based on enhanced electrochemiluminescence by vertically ordered mesoporous silica-nanochannel film. *Front. Chem.* 10, 851178. doi:10.3389/fchem.2022.851178

Ma, X., Liao, W., Zhou, H., Tong, Y., Yan, F., Tang, H., et al. (2020). Highly sensitive detection of rutin in pharmaceuticals and human serum using ITO electrodes modified with vertically-ordered mesoporous silica-graphene nanocomposite films. *J. Mat. Chem. B* 8, 10630–10636. doi:10.1039/d0tb01996h

O'Shannessy, D. J., Yu, G., Smale, R., Fu, Y., Singhal, S., Thiel, R. P., et al. (2012). Folate receptor alpha expression in lung cancer: diagnostic and prognostic significance. *Oncotarget* 3, 414–425. doi:10.18632/oncotarget.519

Scaranti, M., Cojocaru, E., Banerjee, S., and Banerji, U. (2020). Exploiting the folate receptor alpha in oncology. *Nat. Rev. Clin. Oncol.* 17, 349–359. doi:10.1038/s41571-020-0339-5

Soleymani, J., Hasanzadeh, M., Shadjou, N., Somi, M. H., and Jouyban, A. (2020). Spectrofluorimetric cytosensing of colorectal cancer cells using terbium-doped dendritic fibrous nano-silica functionalized by folic acid: a novel optical cytosensor for cancer detection. *J. Pharm. Biomed. Anal.* 180, 113077. doi:10.1016/j.jpba.2019.113077

Soleymani, J., Hasanzadeh, M., Somi, M. H., Shadjou, N., and Jouyban, A. (2018). Probing the specific binding of folic acid to folate receptor using amino-functionalized mesoporous silica nanoparticles for differentiation of MCF 7 tumoral cells from MCF 10A. *Biosens. Bioelectron.* 115, 61–69. doi:10.1016/j.bios.2018.05.025

Teng, Y., Shi, J., and Pong, P. W. T. (2019). Sensitive and specific colorimetric detection of cancer cells based on folate-conjugated gold–iron-oxide composite nanoparticles. *ACS Appl. Nano Mat.* 2, 7421–7431. doi:10.1021/acsanm.9b01947

Tepeli, Y., Demir, B., Timur, S., and Anik, U. (2015). An electrochemical cytosensor based on a PAMAM modified glassy carbon paste electrode. *RSC Adv.* 5, 53973–53978. doi:10.1039/c5ra07893h

Wang, R., Di, J., Ma, J., and Ma, Z. (2012). Highly sensitive detection of cancer cells by electrochemical impedance spectroscopy. *Electrochim. Acta* 61, 179–184. doi:10.1016/j.electacta.2011.11.112

Wang, X., Cheng, S., Wang, X., Wei, L., Kong, Q., Ye, M., et al. (2021). pH-Sensitive dye-based nanobioplatform for colorimetric detection of heterogeneous circulating tumor cells. *ACS Sens.* 6, 1925–1932. doi:10.1021/acssensors.1c00314

Weng, J., Zhang, Z., Sun, L., and Wang, J. A. (2011). High sensitive detection of cancer cell with a folic acid-based boron-doped diamond electrode using an AC impedimetric approach. *Biosens. Bioelectron.* 26, 1847–1852. doi:10.1016/j.bios.2010.01.027

Wu, M. S., Sun, X. T., Zhu, M. J., Chen, H. Y., and Xu, J. J. (2015). Mesoporous silica film-assisted amplified electrochemiluminescence for cancer cell detection. *Chem. Comm.* 51, 14072–14075. doi:10.1039/c5cc06229b

Xu, S., Liu, J., Wang, T., Li, H., Miao, Y., Liu, Y., et al. (2013). A simple and rapid electrochemical strategy for non-invasive, sensitive and specific detection of cancerous cell. *Talanta* 104, 122–127. doi:10.1016/j.talanta.2012.11.040

Yan, F., Chen, J., Jin, Q., Zhou, H., Sailjoi, A., Liu, J., et al. (2020a). Fast one-step fabrication of a vertically-ordered mesoporous silica-nanochannel film on graphene for direct and sensitive detection of doxorubicin in human whole blood. *J. Mat. Chem. C* 8, 7113–7119. doi:10.1039/d0tc00744g

Yan, F., Luo, T., Jin, Q., Zhou, H., Sailjoi, A., Dong, G., et al. (2021). Tailoring molecular permeability of vertically-ordered mesoporous silica-nanochannel films on graphene for selectively enhanced determination of dihydroxybenzene isomers in environmental water samples. *J. Hazard. Mat.* 410, 124636. doi:10.1016/j.jhazmat.2020.124636

Yan, F., Ma, X., Jin, Q., Tong, Y., Tang, H., Lin, X., et al. (2020b). Phenylboronic acid-functionalized vertically ordered mesoporous silica films for selective electrochemical determination of fluoride ion in tap water. *Microchim. Acta* 187, 470. doi:10.1007/s00604-020-04422-4

Zhang, D., Ma, F., Zhang, Q., and Zhang, C. (2017). Highly sensitive detection of epidermal growth factor receptor in lung cancer cells by aptamer-based target-/probe-mediated cyclic signal amplification. *Chem. Comm.* 53, 11496–11499. doi:10.1039/c7cc06823a

Zhang, J., Shen, Y., Liu, Y., Hou, Z., Gu, Y., and Zhao, W. (2018). An electrochemiluminescence cytosensor for sensitive detection of HeLa cells based on a signal amplification strategy of Au-NaYF4:Yb,Er nanocomposites. *Analyst* 143, 4199–4205. doi:10.1039/c8an00793d

Zhang, M., Zou, Y., Zhou, X., Yan, F., and Ding, Z. (2022). Vertically-ordered mesoporous silica films for electrochemical detection of Hg(II) ion in pharmaceuticals and soil samples. *Front. Chem.* 10, 952936. doi:10.3389/fchem.2022.952936

Zhang, T., Xu, S., Lin, X., Liu, J., and Wang, K. (2023). Label-free electrochemical aptasensor based on the vertically-aligned mesoporous silica films for determination of aflatoxin B1. *Biosensors* 13, 661. doi:10.3390/bios13060661

Zhou, H., Ma, X., Sailjoi, A., Zou, Y., Lin, X., Yan, F., et al. (2022). Vertical silica nanochannels supported by nanocarbon composite for simultaneous detection of serotonin and melatonin in biological fluids. *Sens. Actuators B Chem.* 353, 131101. doi:10.1016/j.snb.2021.131101

Zhou, X., Han, Q., Zhou, J., Liu, C., and Liu, J. (2023). Reagentless electrochemical detection of tumor biomarker based on stable confinement of electrochemical probe in bipolar silica nanochannel film. *Nanomaterials* 13, 1645. doi:10.3390/nano13101645

Zou, Y., Zhou, X., Xie, L., Tang, H., and Yan, F. (2022). Vertically-ordered mesoporous silica films grown on boron nitride-graphene composite modified electrodes for rapid and sensitive detection of carbendazim in real samples. *Front. Chem.* 10, 939510. doi:10.3389/fchem.2022.939510